

Prolonged mechanical unloading affects cardiomyocyte excitation-contraction coupling, transverse-tubule structure, and the cell surface

Michael Ibrahim,^{*,1} Abeer Al Masri,^{†,1} Manoraj Navaratnarajah,^{*} Urszula Siedlecka,^{*} Gopal K. Soppa,^{*} Alexey Moshkov,^{*} Sara Abou Al-Saud,^{*,†} Julia Gorelik,^{*} Magdi H. Yacoub,^{*} and Cesare M. N. Terracciano^{*,2}

^{*}Imperial College London, Harefield Heart Science Centre and Cardiovascular Sciences, London, UK; and [†]King Saud University College of Medicine, King Fahad Cardiac Center, Riyadh, Saudi Arabia

ABSTRACT Prolonged mechanical unloading (UN) of the heart is associated with detrimental changes to the structure and function of cardiomyocytes. The mechanisms underlying these changes are unknown. In this study, we report the influence of UN on excitation-contraction coupling, Ca²⁺-induced Ca²⁺ release (CICR) in particular, and transverse (t)-tubule structure. UN was induced in male Lewis rat hearts by heterotopic abdominal heart transplantation. Left ventricular cardiomyocytes were isolated from the transplanted hearts after 4 wk and studied using whole-cell patch clamping, confocal microscopy, and scanning ion conductance microscopy (SICM). Recipient hearts were used as control (C). UN reduced the volume of cardiomyocytes by 56.5% compared with C (UN, $n=90$; C, $n=59$; $P<0.001$). The variance of time-to-peak of the Ca²⁺ transients was significantly increased in unloaded cardiomyocytes (UN 227.4 ± 24.9 ms², $n=42$ vs. C 157.8 ± 18.0 ms², $n=40$; $P<0.05$). UN did not alter the action potential morphology or whole-cell L-type Ca²⁺ current compared with C, but caused a significantly higher Ca²⁺ spark frequency (UN 3.718 ± 0.85 events/100 $\mu\text{m}^2/\text{s}$, $n=47$ vs. C 0.908 ± 0.186 events/100 $\mu\text{m}^2/\text{s}$, $n=45$; $P<0.05$). Confocal studies showed irregular distribution of the t tubules (power of the normal t-tubule frequency: UN $8.13\pm 1.12\times 10^5$, $n=57$ vs. C $20.60\pm 3.174\times 10^5$, $n=56$; $P<0.001$) and SICM studies revealed a profound disruption to the openings of the t tubules and the cell surface in unloaded cardiomyocytes. We show that UN leads to a functional uncoupling of the CICR process and identify disruption of the t-tubule-sarcoplasmic reticulum interaction as a possible mechanism.—Ibrahim, M., Al Masri, A., Navaratnarajah, M., Siedlecka, U., Soppa, G. K., Moshkov, A., Abou Al-Saud, S., Gorelik, J., Yacoub, M. H., Terracciano, C. M. N. Prolonged mechanical unloading affects cardiomyocyte excitation-contraction coupling, transverse-tubule structure, and the cell surface. *FASEB J.* 24, 3321–3329 (2010). www.fasebj.org

Key Words: Ca²⁺-induced Ca²⁺ release • scanning ion conductance microscope • confocal microscope

THERE IS BOTH CLINICAL AND experimental evidence that the myocardium is sensitive to mechanical unloading and that when the failing, overloaded heart is mechanically unloaded its function is initially improved (1–3). This has become an important clinical issue because of the use of left ventricular assist devices (LVADs) for the treatment of heart failure. These devices act predominantly by unloading the myocardium and have shown extremely promising results in some clinical trials (1–3). However, the beneficial effects of LVAD treatment on myocardial function seem to diminish after prolonged mechanical unloading, and the clinical recovery obtained is insufficient for device explantation in most patients (4, 5). In experimental models of mechanical unloading, prolonged unloading can impair cardiac function (6), and this may be partly mediated by deranged excitation-contraction coupling (7).

In cardiomyocytes, contraction is initiated by the opening of the voltage-sensitive L-type Ca²⁺ channels, which are more abundant in the transverse (t) tubules (8, 9); the consequent current, I_{Ca,L}, triggers the opening of the ryanodine receptors (RyR), which results in significant sarcoplasmic reticulum (SR) Ca²⁺ release, in a process of Ca²⁺-induced Ca²⁺ release (CICR) (8). It is largely this Ca²⁺ that bathes the contractile machinery and results in contraction (10). In ventricular myocytes, the spatial relationship between the L-type Ca²⁺ channel and RyR is guaranteed by the t tubule (11).

There is growing evidence that alterations in t-tubule structure are an important cause of deterioration in cardiomyocyte function in a range of cardiac disease states (12), including overload (13), sustained tachycardia (14), hyperglycemia (15), heart failure (16, 17), and others. In agreement with their role in guarantee-

¹ These authors contributed equally to this work.

² Correspondence: Harefield Heart Science Centre, Harefield Hospital, Harefield, Middlesex, UB9 6JH UK. E-mail: c.terracciano@imperial.ac.uk
doi: 10.1096/fj.10-156638

ing efficient Ca^{2+} release, regions of t-tubular disruption (18) are spatially colocalized to areas of impaired Ca^{2+} release, and the degree of t-tubular disruption correlates with the severity of impaired Ca^{2+} release (16). It is not known whether the t-tubule network is sensitive to mechanical unloading, but a recent report suggests that t tubules are regulated by stretch-sensitive molecules (19).

Prolonged unloading modifies the electrophysiological parameters of cardiomyocytes, and such changes can be critically important to overall changes in cardiac function (20, 21). It is also known that prolonged unloading of normal hearts can impair some aspects of Ca^{2+} handling with detrimental effects on cardiomyocyte function. The mechanisms underlying this decline are unknown.

In the present study, we hypothesized that Ca^{2+} release in cardiomyocytes is impaired by chronic unloading. This CICR process is defective in failing cells (13, 17, 18, 22). There is evidence that this derangement is caused by a structural uncoupling of L-type Ca^{2+} channels and RyRs due to defects in the t-tubule network (13, 18, 22). It is possible that similar defects underlie the functional impairment of the chronically unloaded heart.

To test this hypothesis, in rat ventricular myocytes undergoing prolonged mechanical unloading, we measured the trigger for Ca^{2+} release (ICa,L), and SR Ca^{2+} release (the whole-cell Ca^{2+} transient and Ca^{2+} sparks). In addition, we investigated the structure of the t-tubule network to identify whether physical uncoupling of the L-type Ca^{2+} channels and RyR might explain their functional uncoupling.

MATERIALS AND METHODS

Syngeneic male Lewis rats (10–12 wk old, ~220 g) were used in all of the experiments. All animal procedures were approved by the UK Home Office and passed local ethics review at Harefield Heart Science Centre.

Heterotopic abdominal heart transplantation

The heart was harvested from the thorax and heterotopically transplanted into the abdomen of an age-matched syngeneic recipient, as described previously (7, 23, 24). In brief, the donor aorta was anastomosed to the recipient abdominal aorta and the donor pulmonary artery to the recipient inferior vena cava.

Cell isolation

Animals were sacrificed 4 wk after heterotopic abdominal transplantation. The recipient's native heart acted as a control. Cardiomyocytes were isolated by standard enzymatic digestion only from the left ventricular (LV) tissue as described previously (25). Cardiomyocytes were used within 6 h, and those for study were selected at random and were only excluded if they did not have a rod-shaped appearance. All subsequent recordings were performed with cells superfused with normal Tyrode's solution (140 mM NaCl, 6 mM KCl, 1 mM MgCl_2 , 1 mM CaCl_2 , 10 mM glucose, and 10 mM HEPES,

adjusted to pH 7.4 with 2 M NaOH) unless otherwise indicated.

Electrophysiological parameters

Cells were studied using an Axon 2B amplifier (Axon Instruments, Union City, CA, USA) in discontinuous (switch clamp) mode. The pipette resistance was ~30 M Ω , and the pipette filling solution contained 2000 mM KCl, 5 mM HEPES, and 0.1 mM EGTA (pH 7.2). Action potentials (APs) were measured in current-clamp mode after stimulation at 1, 3, and 5 Hz using a 1-ms, 1.2- to 1.4-nA pulse. Times to 50 and 90% repolarization were measured from the stimulation pulse. ICa,L was measured in voltage-clamp mode as described previously (24). The pipette resistance was ~2–3 M Ω , and the pipette-filling solution contained the following: 115 mM cesium aspartate, 20 mM tetraethylammonium chloride, 10 mM EGTA, 10 mM HEPES, and 5 mM MgATP, pH 7.2. The external solution contained the following: 140 mM NaCl, 10 mM glucose, 10 mM HEPES, 1 mM CaCl_2 , 1 mM MgCl_2 , and 6 mM CsCl, pH 7.4. Current-voltage relationships for L-type Ca^{2+} current were built using 450-ms depolarization steps from a holding potential of -40 mV (range -40 to +40 mV, in 5-mV increments) at 1 Hz. Then 200 μM Cd^{2+} was applied, and the protocol was repeated. Subtracted currents obtained were normalized to cell capacitance. All experiments were conducted at 37°C.

Imaging of t tubules

Confocal microscopy

The membrane-binding dye, di-8-ANEPPS (Molecular Probes, Eugene, OR, USA) was used. Di-8-ANEPPS (10 μM) was added to a suspension of isolated cells for 10 min. The experimental chamber was mounted on the stage of a Zeiss Axiovert microscope (Carl Zeiss, Oberkochen, Germany) with an LSM 510 confocal attachment, and myocytes were observed through a Zeiss EC Plan-NeoFluar $\times 40$ oil-immersion lens (numerical aperture 1.3). Di-8-ANEPPS was excited using the 488-nm line of an argon laser, and the emitted fluorescence was collected through a 505-nm long-pass filter. A focal plane that excluded the nuclei was selected for high-resolution imaging of the t-tubule structure. Lower resolution Z-stack images of the same cells were used to assess the size and shape of cardiomyocytes. Z-stack images were analyzed using a custom-written macro in ImageJ (U.S. National Institutes of Health; <http://rsb.info.nih.gov/ij/>) to measure cell volume. High-resolution images were converted to binary images using the autothreshold function of ImageJ. This involves serial divisions of the "top" and "bottom" ends of the range of foreground and background pixel intensities. These binary images were used to generate plot profiles, which were analyzed in MATLAB (The MathWorks, Inc., Natick, MA, USA) using a custom-written macro to calculate the Fourier transform of the di-8-ANEPPS signal (26). The peak of the power-frequency relationship was calculated for each image and compared between the control and unloaded groups. The amplitude of the peak is taken as an index of regular distribution of the t-tubule network, as previously suggested (26).

Scanning ion conductance microscope (SICM)

The SICM setup has been described previously (27, 28). This uses a micropipette which scans close to the cell surface. The proximity to the cell surface alters the resistance of the

micropipette and therefore current flow. Changes in current are used to produce a detailed image of the cell surface (27, 28). This allows visualization of the openings of the t tubules at the cell surface without disrupting its detailed architecture and has been used to characterize t-tubule disruption and other surface changes in heart failure (17). We used hopping probe ion conductance microscopy without continuous feedback (29). We obtained high-resolution images of the surface of freshly isolated LV cardiomyocytes from either control or unloaded hearts. In all SICM experiments, micropipettes and the bath solution contained the same physiological L-15 medium (Life Technologies, Inc., Parsippany, NJ), so that salt concentration gradient potentials and liquid junction potentials were not generated.

To quantify the data obtained during scanning we introduced an index of the completeness of the Z grooves on the surface of cardiomyocytes (Z-groove index). The Z groove describes the domes and troughs of the surface of cardiomyocytes, and t-tubule openings are known to sit in these Z-grooves (30). To calculate the Z-groove index, we measured the maximum extent of Z grooves observed on single SICM images and divided this length by the total estimated Z-groove length, as if they extended across the whole surface, guided by the structure of normal SICM images as described previously (30).

Imaging of Ca²⁺ sparks and transients

The Ca²⁺-sensitive fluorescent dye fluo-4 AM (Molecular Probes) was used to monitor local changes in Ca²⁺ concentration. Aliquots of cells were incubated with fluo-4 AM (10 μM) for 20 min, and this mixture was allowed to de-esterify for at least 30 min before cells were used. Cells were studied with the same confocal microscope described above. After a period of 30 s of quiescence, line scans were collected. Analysis was performed using custom-written routines in MATLAB R2006b (The MathWorks, Inc.) following the threshold-based algorithm for automatic Ca²⁺ spark detection of Cheng *et al.* (31). Detection criteria for Ca²⁺ sparks were set at 3.8 sd above the background noise. Ca²⁺ spark frequency was obtained from the line scans, and Ca²⁺ spark amplitude was defined as the peak fluorescence over background fluorescence (F/F_0). Morphometric analysis of Ca²⁺ sparks elucidated the full width at half-maximum (FWHM) and full duration at half-maximum (FDHM). To examine the Ca²⁺ transient, cells were field-stimulated at 1 Hz, and a line scan was performed, as described previously (32). We measured time to peak

amplitude and variance of time to peak amplitude. Time to relaxation was measured as the time from the peak of the Ca²⁺ transient to 50% decline.

Statistical analysis

Statistical analysis was performed using the nonparametric Mann-Whitney test, except where indicated. The analysis was performed using Prism4 software (GraphPad Software Inc., San Diego, CA, USA). $P < 0.05$ was taken as significant.

RESULTS

Prolonged unloading reduces cell size

The volume of cardiomyocytes from chronically unloaded (UN) hearts was 56.5% smaller than that for control (C) hearts (UN $19,190 \pm 779 \mu\text{m}^3$, $n=90$ vs. C $44,120 \pm 2042 \mu\text{m}^3$, $n=59$; $P < 0.001$). This reduction in cell size was confirmed by a reduced cell capacitance measured during the electrophysiological experiments (Fig. 1).

Ca²⁺ transient is altered by prolonged unloading

To test whether prolonged unloading of the left ventricle altered the Ca²⁺ transient, we field-stimulated isolated cells loaded with fluo-4 AM. In cells from the chronically unloaded heart, the average time to peak was significantly longer (UN 41.8 ± 2.5 ms, $n=42$ vs. C 30.9 ± 1.3 ms, $n=40$; $P < 0.0005$) as was the time to 50% decline (UN 150.6 ± 10.5 ms, $n=42$ vs. C 90.4 ± 2.8 ms, $n=40$; $P < 0.0001$) compared with control cells. The peak amplitude of the whole-cell Ca²⁺ transient was significantly smaller in cells from the chronically unloaded heart compared with control heart (UN $3.70 \pm 0.21 F/F_0$, $n=42$ vs. C $5.22 \pm 0.26 F/F_0$, $n=40$; $P < 0.0001$). The variance of time-to-peak of the Ca²⁺ transients was significantly increased in unloaded cardiomyocytes (UN $227.4 \pm 24.9 \text{ ms}^2$, $n=42$ vs. C $157.8 \pm 18 \text{ ms}^2$, $n=40$; $P < 0.05$), suggesting that the

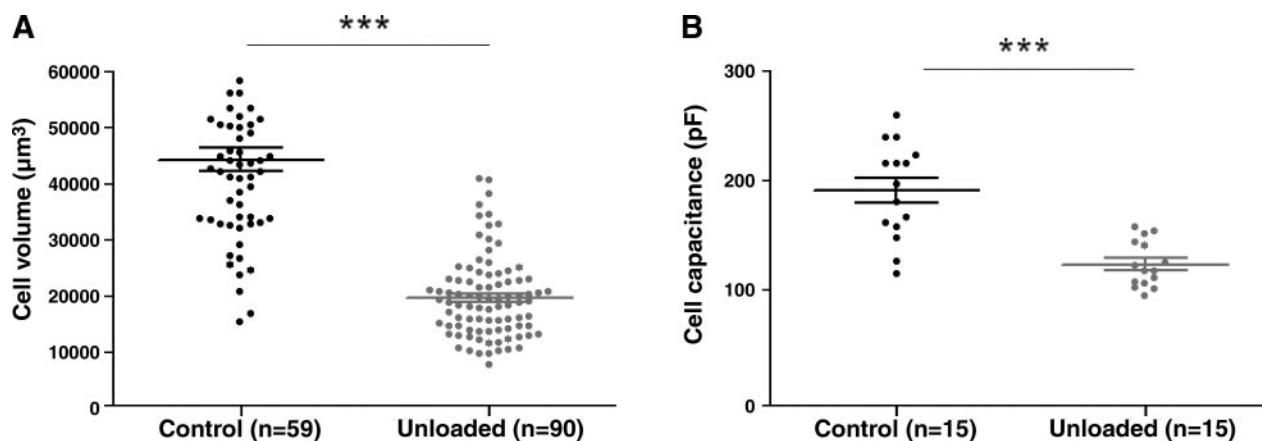


Figure 1. Prolonged mechanical unloading reduces cell size. *A*) Cell volumes were assessed by analysis of di-8-ANEPPS images. Unloaded cell volumes were significantly smaller than control cell volumes. *B*) Cell capacitance measurements confirmed the reduction in cell volume after chronic unloading.

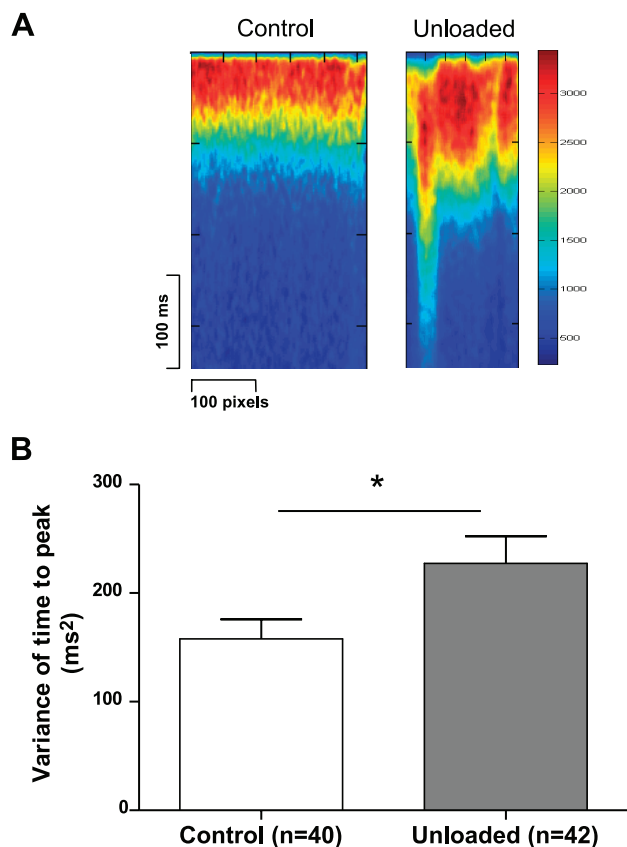


Figure 2. Prolonged mechanical unloading disrupts the Ca^{2+} transient. *A*) Two representative traces showing that the whole-cell Ca^{2+} transient, measured in line-scan mode during confocal experiments, is less synchronous in unloaded than in control cells. *B*) The average variance of the time to peak Ca^{2+} transient is more variable in line scans of unloaded compared with control cells. This result indicates less synchronous Ca^{2+} release across the whole cell.

synchronicity of Ca^{2+} release was disrupted (**Fig. 2**). Possible causes for this impaired Ca^{2+} release include altered L-type Ca^{2+} channel function, altered RYR function, or an uncoupling of the CICR machinery.

L-type Ca^{2+} current density is unaffected and inactivation is delayed

We measured the whole-cell $\text{I}_{\text{Ca,L}}$ in control ($n=15$) and unloaded ($n=15$) LV cardiomyocytes. There was no difference in the current density-voltage relationship of this channel between groups (**Fig. 3A, B**). Given that cell capacitance was reduced in the smaller unloaded cells, absolute current amplitude declined in proportion to cell size. Thus, the trigger for SR Ca^{2+} release was not altered by prolonged mechanical unloading under voltage clamping conditions. The fast inactivation of the L-type Ca^{2+} current was significantly slower in unloaded cardiomyocytes (**Fig. 3C**) (UN 16.29 ± 0.42 ms, $n=15$ vs. C 13.82 ± 0.71 ms, $n=15$; $P < 0.01$). This may be due to slower Ca^{2+} release from the SR.

AP is unaffected

Because the synchronicity of the Ca^{2+} transient may be affected by AP morphology, we recorded APs from unloaded and control myocytes. The resting membrane potential was unaffected by prolonged mechanical unloading (UN -62.51 ± 0.001 mV, $n=16$ vs. C -61.08 ± 0.002 mV, $n=8$; NS). The time to 50% repolarization was similarly unchanged (UN 74.08 ± 11.34 ms, $n=16$ vs. 66.38 ± 4.01 ms, $n=8$; NS), as was the time to 90% repolarization (UN 151.6 ± 25.22 ms, $n=16$ vs. C 158.5 ± 8.926 ms, $n=8$; NS). Thus, chronic mechanical unloading did not alter the AP of LV cardiomyocytes (**Fig. 3D**).

Taken together, these results suggest that there is a local disruption of CICR in unloaded cardiomyocytes, which is not due to altered L-type Ca^{2+} channel activity. To investigate the basis of this impaired Ca^{2+} release, we assessed the components of the local CICR process, which include RyR and the t-tubular structure.

Prolonged mechanical unloading alters the Ca^{2+} spark frequency and morphology

Ca^{2+} sparks are the elementary SR Ca^{2+} release events and can be used to investigate RyR function in intact, quiescent cells (33). We measured Ca^{2+} sparks from both control and unloaded hearts (**Fig. 4**). Unloaded cells showed a significantly higher Ca^{2+} spark frequency (UN 3.718 ± 0.85 events/100 $\mu\text{m}/\text{s}$, $n=47$ vs. C 0.908 ± 0.186 events/100 $\mu\text{m}/\text{s}$, $n=45$; $P < 0.05$). In unloaded cardiomyocytes, Ca^{2+} spark width (UN 3.312 ± 0.066 μm , $n=410$ vs. C 2.689 ± 0.043 μm , $n=149$; $P < 0.001$) and duration (UN 25.87 ± 0.825 ms, $n=410$ vs. C 14.85 ± 0.453 ms, $n=149$; $P < 0.001$) were increased, whereas Ca^{2+} spark peak was decreased (UN 1.517 ± 0.01211 , $n=410$ vs. C 1.724 ± 0.02408 , $n=149$; $P < 0.0001$). These results indicate altered activity of the RyR. We have reported previously that the SR Ca^{2+} content is unchanged in unloading myocytes (7); thus, we investigated whether the changes in Ca^{2+} sparks might be due to alterations at the level of the structural coupling of the RyR and L-type Ca^{2+} channels at the t tubules.

Prolonged mechanical unloading disrupts the t tubules

We investigated the t-tubule network in cells from the chronically unloaded heart because changes in SR Ca^{2+} release have been associated with t-tubule disruption (18, 34). To do this, we stained cells with the membrane-staining dye di-8-ANEPPS (**Fig. 5A**). Unloading did not alter the density of the t-tubule network (**Fig. 5B**), consistent with an unchanged $\text{I}_{\text{Ca,L}}$, but significantly reduced its regularity (**Fig. 5C, D**), with fewer t tubules lying in their ordinary position.

To image the external membrane structure and its relationship with the t-tubule network at high resolution in living cells, we used SICM. SICM imaging of unloaded cells showed changes on the cardiomyocyte

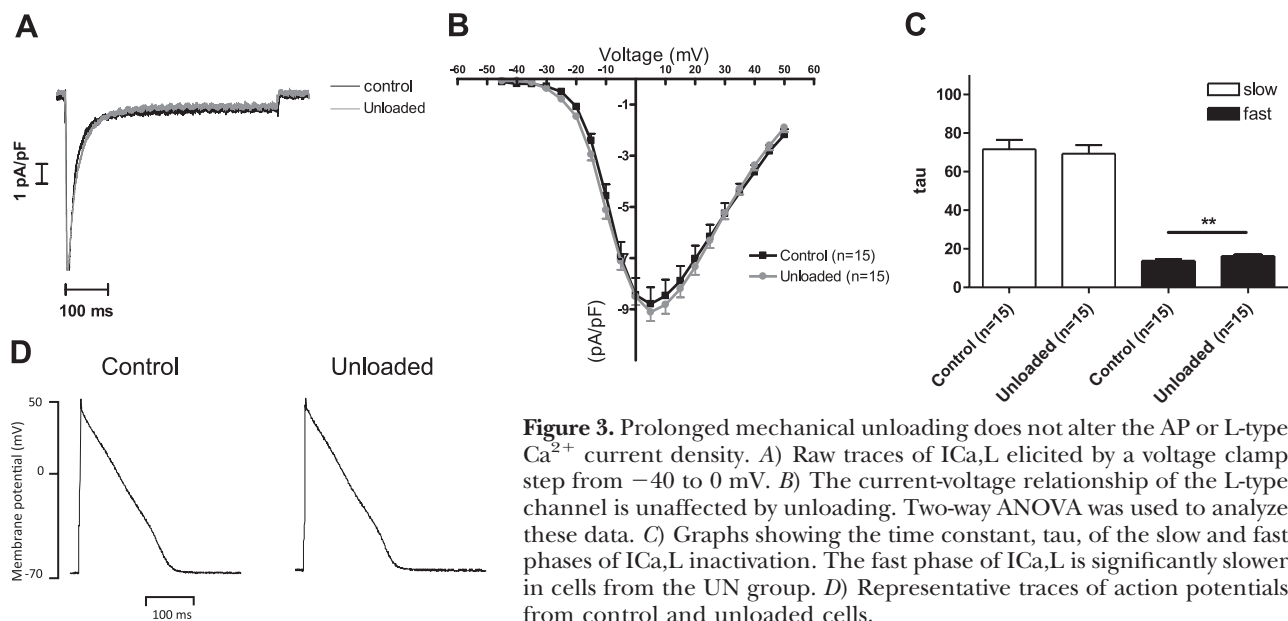


Figure 3. Prolonged mechanical unloading does not alter the AP or L-type Ca^{2+} current density. *A*) Raw traces of $\text{I}_{\text{Ca,L}}$ elicited by a voltage clamp step from -40 to 0 mV. *B*) The current-voltage relationship of the L-type channel is unaffected by unloading. Two-way ANOVA was used to analyze these data. *C*) Graphs showing the time constant, τ , of the slow and fast phases of $\text{I}_{\text{Ca,L}}$ inactivation. The fast phase of $\text{I}_{\text{Ca,L}}$ is significantly slower in cells from the UN group. *D*) Representative traces of action potentials from control and unloaded cells.

surface and a decrease in the Z-groove index compared with control cells (UN 0.3841 ± 0.02451 , $n=17$ vs. 0.8040 ± 0.03513 , $n=10$; $P < 0.0001$) (Fig. 6). We found that the t-tubule network was less regular in unloaded compared with control cells, with a smaller proportion of t-tubule openings in their ordinary position relative to control cells, defined by our parameter, the Z groove, as described previously (30).

DISCUSSION

In the present study, we show that cardiomyocytes from chronically unloaded hearts have impaired Ca^{2+} re-

lease and increased asynchronous Ca^{2+} release events, despite intact Ca^{2+} triggers (normal $\text{I}_{\text{Ca,L}}$). Cells from chronically unloaded hearts also have disrupted t-tubule structure, with a normal density but abnormal pattern. The disrupted, asynchronous Ca^{2+} release events can be explained by a structural and functional uncoupling of the RyRs and L-type channels (22). This is a fundamental mechanism for impaired contractility and arrhythmia in heart failure, and we show this for the first time in the chronically unloaded heart. We suggest that this mechanism may contribute to explaining the regression of improved contractility observed in patients treated chronically with LVADs.

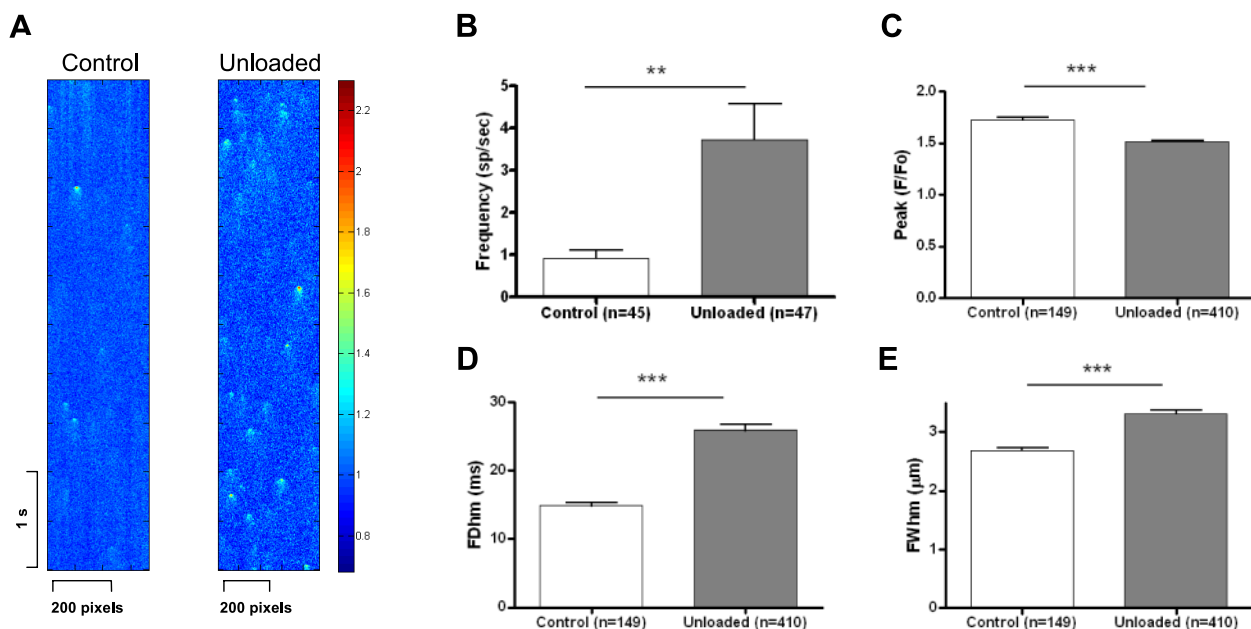


Figure 4. Ca^{2+} spark properties are altered by prolonged mechanical unloading. *A*) Representative images of Ca^{2+} sparks in resting cells during line scanning. *B–D*) Cells from the chronically unloaded heart have more frequent Ca^{2+} sparks (*B*), which are smaller in amplitude (*C*), longer in duration (*D*), and wider (*E*).

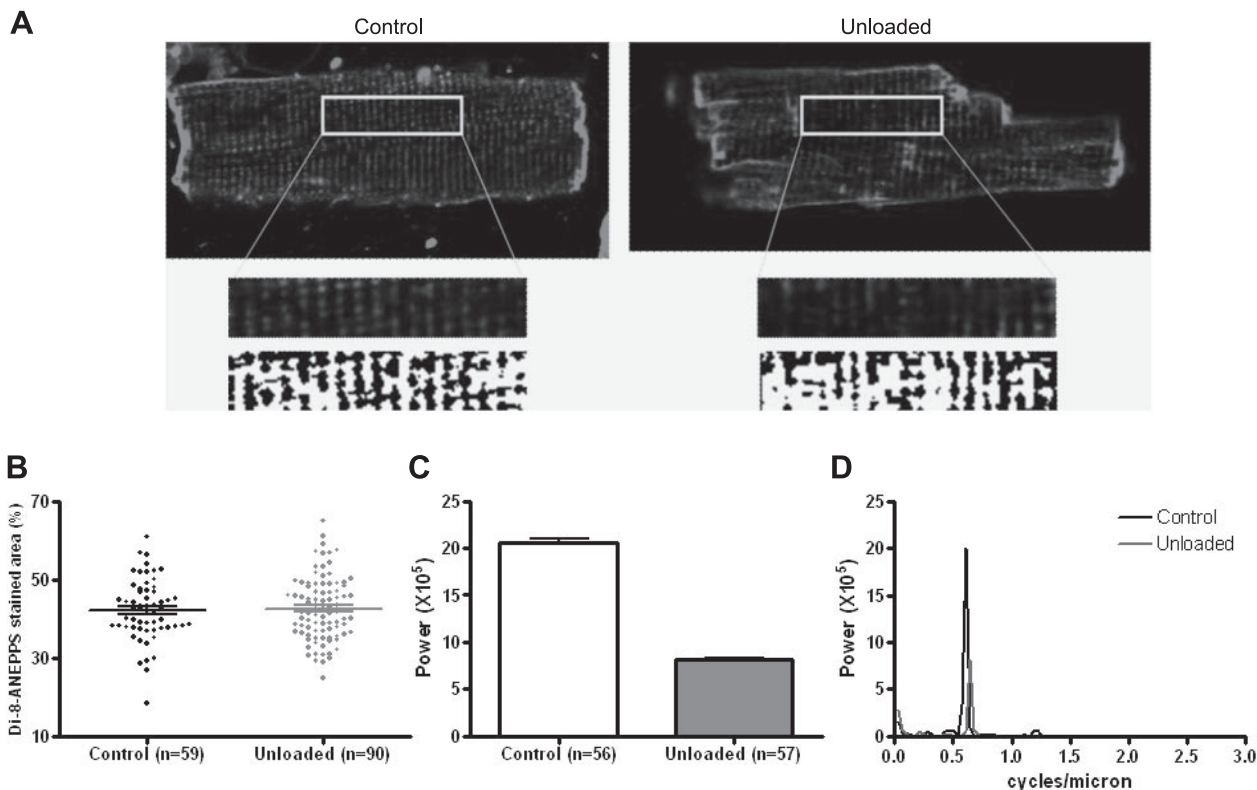


Figure 5. Prolonged mechanical unloading disrupts the t-tubule structure. *A*) Representative images of di-8-ANEPPS-stained cardiomyocytes from chronically unloaded and control hearts. Binary images of the central area indicate that the t tubules of unloaded cells are significantly disrupted. Length of the inset is 40 μm . *B*) The density of the t-tubule network was assessed by the percentage of the cell interior stained with di-8-ANEPPS, and this parameter was unchanged between control and unloaded cells. *C, D*) Fourier analysis of the binary di-8-ANEPPS images revealed that the peak corresponding to the normal frequency of the t tubules was far less powerful in unloaded cells than in control cells. This indicates that the t tubules were not arranged in their normal periodic manner but rather were scattered at abnormal positions throughout the cell.

One unexpected result was that despite alterations to the Ca^{2+} transient, the AP morphology was not altered (35). In rat myocytes, SR Ca^{2+} uptake is almost entirely responsible for Ca^{2+} extrusion, with a much smaller role for the $\text{Na}^+/\text{Ca}^{2+}$ exchanger (NCX) (36). For this reason NCX inward current is smaller and would therefore have less effect on AP shape. Although changes in AP duration have been reported after large cytoplasmic $[\text{Ca}^{2+}]$ changes in rat cardiomyocytes (35), it is possible that the changes in our experiments were too small to result in significant changes in AP shape.

CICR uncoupling

There is accumulating evidence that t-tubule disruption produces an uncoupling of L-type Ca^{2+} channels (which are concentrated in the t tubule) and the RyR (in the SR) in overload (11, 18, 22, 37). The “orphaned” RyRs no longer respond to L-type Ca^{2+} channel opening because they are functionally uncoupled by their distance and become less sensitive to the local increases in $[\text{Ca}^{2+}]$. We speculate that this is also the case in the chronically unloaded heart. This uncoupling is evidenced by the increased variance in the time-to-peak of the stimulated Ca^{2+} transient and the

increased spark frequency, and a structural basis is suggested by the disruptions to the t-tubule network. The changes to the parameters of Ca^{2+} spark mass (FWHM and FDHM) may be dependent on a number of mechanisms, including properties of Ca^{2+} diffusion through the cell, and altered opening features of individual RyR in each cluster (38). We have ruled out increased SR Ca^{2+} content as a mechanism for increasing the Ca^{2+} spark frequency because we previously reported that chronic mechanical unloading did not alter the SR Ca^{2+} content (7). Our suggestion that the deranged Ca^{2+} release is due to a structural abnormality in the t tubules is supported by evidence that the points of delayed Ca^{2+} release spatially relate to defects in the t-tubule network in other studies (7, 18, 34, 39). Whether there is RyR–L-type Ca^{2+} channel uncoupling at those points is not known, but this is likely to be the case (22). However, it is important to note that some RyR uncoupling is normal and occurs in some parts of atrial and ventricular cells (40, 41). However, the function of these solitary RyRs appear to be distinct from CICR, and tight RyR and L-type Ca^{2+} channel localization is necessary for effective CICR (42, 43).

The CICR uncoupling may explain in part the impaired contractility of normal chronically unloaded

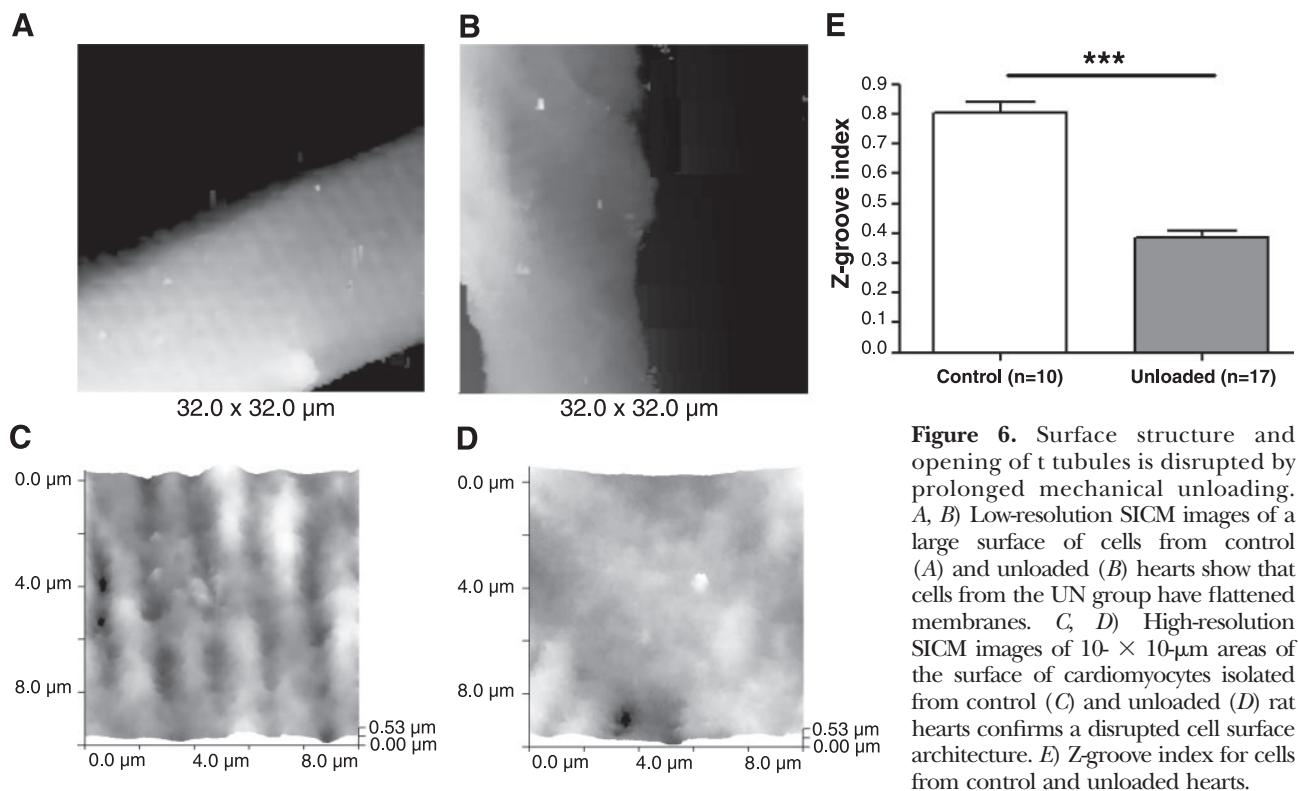


Figure 6. Surface structure and opening of t tubules is disrupted by prolonged mechanical unloading. *A, B* Low-resolution SICM images of a large surface of cells from control (*A*) and unloaded (*B*) hearts show that cells from the UN group have flattened membranes. *C, D* High-resolution SICM images of $10 \times 10\text{-}\mu\text{m}$ areas of the surface of cardiomyocytes isolated from control (*C*) and unloaded (*D*) rat hearts confirms a disrupted cell surface architecture. *E* Z-groove index for cells from control and unloaded hearts.

ventricular cardiomyocytes we described in our previous study (7). We also identified a reduced myofilament sensitivity to Ca^{2+} in that study, which can play a causal role in impairing whole-cell contractility. This is also common to heart failure.

T-tubule physiology

The t tubule is the structural basis of the CICR coupling mechanism (11). Delayed SR Ca^{2+} release in cardiomyocytes has been correlated to gaps in the t-tubule system, both in normal and failing ventricular cardiomyocytes (18, 39). T-tubule disruption also correlates with the degree of heart failure (34). Thus, there appears to be a tight connection between disrupted t-tubule structure and defective Ca^{2+} handling. This has been demonstrated as an important mechanism after pathological insults to the myocardium, including overload (13, 22), sustained tachycardia (14), hyperglycemia (15), ischemia (17, 18), and dilated and hypertrophic cardiomyopathy (17). Here, we add chronic unloading to the list of stressors to which the t-tubule structure is sensitive.

Short-term and long-term unloading

Short-term mechanical unloading has been associated with improved function in normal (44) and failing hearts (6). The improved function has also been demonstrated clinically (2, 45–47). The mechanisms mediating improved function span the spectrum of cardiac physiology and include improved Ca^{2+} handling (20, 48, 49). It is not yet known whether the initial func-

tional improvements after mechanical unloading are mediated by effects on the t-tubule network.

Prolonged unloading is associated with impaired function and Ca^{2+} handling in the normal (50) and failing hearts (6, 51). These data correlate with the observed biphasic response of cardiac function after LVAD implantation in patients with heart failure (4). Maybaum *et al.* (4) show that cardiac function is initially increased, as the overload is removed. However, with prolonged unloading cardiac function begins to decrease again. The mechanisms mediating this are not clear, but a recent clinical report highlights initial improvements in Ca^{2+} cycling (after LVAD therapy in patients with heart failure), including the expression of a number of Ca^{2+} -handling proteins, followed by subsequent impairment in Ca^{2+} homeostasis with prolonged unloading (51).

It is difficult to compare the period of mechanical unloading investigated here with those that would be used clinically, as the time course of the response is clearly very different. We used a period of 4 wk because previous studies indicated that this produced an atrophic response (6, 7).

We described the functional impairment of chronically unloaded normal hearts previously and identified reduced myofilament sensitivity to Ca^{2+} as an important mechanism (7). Our present results indicate that t-tubule dysfunction plays a role in the pathogenesis of impaired contractility of the chronically unloaded heart.

One limitation of our study is that our experiments were not performed with failing hearts, and the possibility remains that the subsequent decline in chronically unloaded failing hearts represents a return of the failing

phenotype after an initial functional improvement due to unloading. Nevertheless, our results indicate that chronic unloading alone can significantly impair Ca^{2+} regulation of cardiomyocytes and, in particular, the CICR mechanism.

An additional limitation is that the heterotopic abdominal transplantation model differs in several respects from the conditions of LVADs. The experimentally unloaded heart is denervated, and the intra-abdominal pressures are very different from the intrathoracic pressures. These differences represent a limit to the comparability of the model to the LVAD.

We conclude that prolonged mechanical unloading of normal hearts impairs CICR in cardiomyocytes due to impairment of the SR Ca^{2+} release process. T-tubular disarray may be the structural basis of the impaired CICR we observed. These results may explain the deleterious effects of prolonged mechanical unloading in experimental studies and the regression of functional improvements in clinical studies. FJ

This work was supported by a British Heart Foundation M.B.-Ph.D. studentship to M.I. (FS/09/025/27468).

REFERENCES

1. Yacoub, M. H. (2001) A novel strategy to maximize the efficacy of left ventricular assist devices as a bridge to recovery. *Eur. Heart J.* **22**, 534–540
2. Birks, E. J., Tansley, P. D., Hardy, J., George, R. S., Bowles, C. T., Burke, M., Banner, N. R., Khaghani, A., and Yacoub, M. H. (2006) Left ventricular assist device and drug therapy for the reversal of heart failure. *N. Engl. J. Med.* **355**, 1873–1884
3. Dandel, M., Weng, Y., Siniawski, H., Potapov, E., Lehmkühl, H. B., and Hetzer, R. (2005) Long-term results in patients with idiopathic dilated cardiomyopathy after weaning from left ventricular assist devices. *Circulation* **112**, 137–145
4. Maybaum, S., Mancini, D., Xydas, S., Starling, R. C., Aaronson, K., Pagani, F. D., Miller, L. W., Margulies, K., McRee, S., Frazier, O. H., and Torre-Amione, G. (2007) Cardiac improvement during mechanical circulatory support: a prospective multicenter study of the LVAD Working Group. *Circulation* **115**, 2497–2505
5. Mancini, D. M., Beniaminovit, A., Levin, H., Catanese, K., Flannery, M., DiTullio, M., Savin, S., Cordisco, M. E., Rose, E., and Oz, M. (1998) Low incidence of myocardial recovery after left ventricular assist device implantation in patients with chronic heart failure. *Circulation* **98**, 2383–2389
6. Oriyanhan, W., Tsuneyoshi, H., Nishina, T., Matsuoka, S., Ikeda, T., and Komeda, M. (2007) Determination of optimal duration of mechanical unloading for failing hearts to achieve bridge to recovery in a rat heterotopic heart transplantation model. *J. Heart Lung Transplant.* **26**, 16–23
7. Soppa, G. K., Lee, J., Stagg, M. A., Siedlecka, U., Youssef, S., Yacoub, M. H., and Terracciano, C. M. (2008) Prolonged mechanical unloading reduces myofilament sensitivity to calcium and sarcoplasmic reticulum calcium uptake leading to contractile dysfunction. *J. Heart Lung Transplant.* **27**, 882–889
8. Bers, D. M. (2002) Cardiac excitation-contraction coupling. *Nature* **415**, 198–205
9. Gu, Y., Gorelik, J., Spohr, H. A., Shevchuk, A. I., Lab, M., Harding, S., Vodyanoy, I., Klenerman, D., and Korchev, Y. (2002) High resolution scanning patch-clamp: new insights into cell function. *FASEB J.* **16**, 748–450
10. Bers, D. M. (1991) *Excitation-Contraction Coupling and Cardiac Contractile Force*, Kluwer Academic Publishers, Dordrecht, The Netherlands

11. Orchard, C., and Brette, F. (2008) t-Tubules and sarcoplasmic reticulum function in cardiac ventricular myocytes. *Cardiovasc. Res.* **77**, 237–244
12. Brette, F., and Orchard, C. (2003) T-tubule function in mammalian cardiac myocytes. *Circ. Res.* **92**, 1182–1192
13. Gomez, A. M., Valdivia, H. H., Cheng, H., Lederer, M. R., Santana, L. F., Cannell, M. B., McCune, S. A., Altschuld, R. A., and Lederer, W. J. (1997) Defective excitation-contraction coupling in experimental cardiac hypertrophy and heart failure. *Science* **276**, 800–806
14. He, J., Conklin, M. W., Foell, J. D., Wolff, M. R., Haworth, R. A., Coronado, R., and Kamp, T. J. (2001) Reduction in density of transverse tubules and L-type Ca^{2+} channels in canine tachycardia-induced heart failure. *Cardiovasc. Res.* **49**, 298–307
15. Stolen, T. O., Hoydal, M. A., Kemi, O. J., Catalucci, D., Ceci, M., Aasum, E., Larsen, T., Rolim, N., Condorelli, G., Smith, G. L., and Wisloff, U. (2009) Interval training normalizes cardiomyocyte function, diastolic Ca^{2+} control, and SR Ca^{2+} release synchronicity in a mouse model of diabetic cardiomyopathy. *Circ. Res.* **105**, 527–536
16. Louch, W. E., Bito, V., Heinzel, F. R., Macianskiene, R., Vanhaecke, J., Flameng, W., Mubagwa, K., and Sipido, K. R. (2004) Reduced synchrony of Ca^{2+} release with loss of T-tubules—a comparison to Ca^{2+} release in human failing cardiomyocytes. *Cardiovasc. Res.* **62**, 63–73
17. Lyon, A. R., MacLeod, K. T., Zhang, Y., Garcia, E., Kanda, G. K., Lab, M. J., Korchev, Y. E., Harding, S. E., and Gorelik, J. (2009) Loss of T-tubules and other changes to surface topography in ventricular myocytes from failing human and rat heart. *Proc. Natl. Acad. Sci. U. S. A.* **106**, 6854–6859
18. Heinzel, F. R., Bito, V., Biesmans, L., Wu, M., Detre, E., von, W. F., Claus, P., Dymarkowski, S., Maes, F., Bogaert, J., Rademakers, F., D'hooge, J., and Sipido, K. (2008) Remodeling of T-tubules and reduced synchrony of Ca^{2+} release in myocytes from chronically ischemic myocardium. *Circ. Res.* **102**, 338–346
19. Zhang, R., Yang, J., Zhu, J., and Xu, X. (2009) Depletion of zebrafish Tcap leads to muscular dystrophy via disrupting sarcomere-membrane interaction, not sarcomere assembly. *Hum. Mol. Genet.* **18**, 4130–4140
20. Terracciano, C. M., Hardy, J., Birks, E. J., Khaghani, A., Banner, N. R., and Yacoub, M. H. (2004) Clinical recovery from end-stage heart failure using left-ventricular assist device and pharmacological therapy correlates with increased sarcoplasmic reticulum calcium content but not with regression of cellular hypertrophy. *Circulation* **109**, 2263–2265
21. Zafeiridis, A., Jeevanandam, V., Houser, S. R., and Margulies, K. B. (1998) Regression of cellular hypertrophy after left ventricular assist device support. *Circulation* **98**, 656–662
22. Song, L. S., Sobie, E. A., McCulle, S., Lederer, W. J., Balke, C. W., and Cheng, H. (2006) Orphaned ryanodine receptors in the failing heart. *Proc. Natl. Acad. Sci. U. S. A.* **103**, 4305–4310
23. Ono, K., and Lindsey, E. S. (1969) Improved technique of heart transplantation in rats. *J. Thorac. Cardiovasc. Surg.* **57**, 225–229
24. Soppa, G. K., Lee, J., Stagg, M. A., Felkin, L. E., Barton, P. J., Siedlecka, U., Youssef, S., Yacoub, M. H., and Terracciano, C. M. (2008) Role and possible mechanisms of clenbuterol in enhancing reverse remodeling during mechanical unloading in murine heart failure. *Cardiovasc. Res.* **77**, 695–706
25. Siedlecka, U., Arora, M., Kolettis, T., Soppa, G. K., Lee, J., Stagg, M. A., Harding, S. E., Yacoub, M. H., and Terracciano, C. M. (2008) Effects of clenbuterol on contractility and Ca^{2+} homeostasis of isolated rat ventricular myocytes. *Am. J. Physiol. Heart Circ. Physiol.* **295**, H1917–H1926
26. Swift, F., Birkeland, J. A., Tovsrud, N., Enger, U. H., Aronsen, J. M., Louch, W. E., Sjaastad, I., and Sejersted, O. M. (2008) Altered $\text{Na}^+/\text{Ca}^{2+}$ -exchanger activity due to downregulation of Na^+/K^+ -ATPase α_2 -isoform in heart failure. *Cardiovasc. Res.* **78**, 71–78
27. Korchev, Y. E., Milovanovic, M., Bashford, C. L., Bennett, D. C., Sviderskaya, E. V., Vodyanoy, I., and Lab, M. J. (1997) Specialized scanning ion-conductance microscope for imaging of living cells. *J. Microsc.* **188**, 17–23
28. Korchev, Y. E., Raval, M., Lab, M. J., Gorelik, J., Edwards, C. R., Rayment, T., and Klenerman, D. (2000) Hybrid scanning ion conductance and scanning near-field optical microscopy for the study of living cells. *Biophys. J.* **78**, 2675–2679
29. Novak, P., Li, C., Shevchuk, A. I., Stepanyan, R., Caldwell, M., Hughes, S., Smart, T. G., Gorelik, J., Ostanin, V. P., Lab, M. J., Moss, G. W., Frolenkov, G. I., Klenerman, D., and Korchev, Y. E.

- (2009) Nanoscale live-cell imaging using hopping probe ion conductance microscopy. *Nat. Methods* **6**, 279–281
30. Gorelik, J., Yang, L. Q., Zhang, Y., Lab, M., Korchev, Y., and Harding, S. E. (2006) A novel Z-groove index characterizing myocardial surface structure. *Cardiovasc. Res.* **72**, 422–429
 31. Cheng, H., Song, L. S., Shirokova, N., Gonzalez, A., Lakatta, E. G., Rios, E., and Stern, M. D. (1999) Amplitude distribution of calcium sparks in confocal images: theory and studies with an automatic detection method. *Biophys. J.* **76**, 606–617
 32. Stagg, M. A., Carter, E., Sohrabi, N., Siedlecka, U., Soppa, G. K., Mead, F., Mohandas, N., Taylor-Harris, P., Baines, A., Bennett, P., Yacoub, M. H., Pinder, J. C., and Terracciano, C. M. (2008) Cytoskeletal protein 4.1R affects repolarization and regulates calcium handling in the heart. *Circ. Res.* **103**, 855–863
 33. Cheng, H., and Lederer, W. J. (2008) Calcium sparks. *Physiol. Rev.* **88**, 1491–1545
 34. Louch, W. E., Mork, H. K., Sexton, J., Stromme, T. A., Laake, P., Sjaastad, I., and Sejersted, O. M. (2006) T-tubule disorganization and reduced synchrony of Ca²⁺ release in murine cardiomyocytes following myocardial infarction. *J. Physiol.* **574**, 519–533
 35. duBell, W. H., Boyett, M. R., Spurgeon, H. A., Talo, A., Stern, M. D., and Lakatta, E. G. (1991) The cytosolic calcium transient modulates the action potential of rat ventricular myocytes. *J. Physiol.* **436**, 347–369
 36. Bassani, J. W. M., Bassani, R. A., and Bers, D. M. (1994) Relaxation in rabbit and rat cardiac cells: species-dependent differences in cellular mechanisms. *J. Physiol.* **476**, 279–293
 37. Lenaerts, I., Bito, V., Heinzel, F. R., Driesen, R. B., Holemans, P., D'hooge, J., Heidbuchel, H., Sipido, K. R., and Willems, R. (2009) Ultrastructural and functional remodeling of the coupling between Ca²⁺ influx and sarcoplasmic reticulum Ca²⁺ release in right atrial myocytes from experimental persistent atrial fibrillation. *Circ. Res.* **105**, 876–885
 38. Wang, S. Q., Wei, C., Zhao, G., Brochet, D. X., Shen, J., Song, L. S., Wang, W., Yang, D., and Cheng, H. (2004) Imaging microdomain Ca²⁺ in muscle cells. *Circ. Res.* **94**, 1011–1022
 39. Meethal, S. V., Potter, K. T., Redon, D., Munoz-del-Rio, A., Kamp, T. J., Valdivia, H. H., and Haworth, R. A. (2007) Structure-function relationships of Ca spark activity in normal and failing cardiac myocytes as revealed by flash photography. *Cell Calcium* **41**, 123–134
 40. Sun, X. H., Protasi, F., Takahashi, M., Takeshima, H., Ferguson, D. G., and Franzini-Armstrong, C. (1995) Molecular architecture of membranes involved in excitation-contraction coupling of cardiac muscle. *J. Cell Biol.* **129**, 659–671
 41. Protasi, F., Sun, X. H., and Franzini-Armstrong, C. (1996) Formation and maturation of the calcium release apparatus in developing and adult avian myocardium. *Dev. Biol.* **173**, 265–278
 42. Stern, M. D. (1992) Theory of excitation-contraction coupling in cardiac muscle. *Biophys. J.* **63**, 497–517
 43. Stern, M. D., and Lakatta, E. G. (1992) Excitation-contraction coupling in the heart: the state of the question. *FASEB J.* **6**, 3092–3100
 44. Ritter, M., Su, Z., Xu, S., Shelby, J., and Barry, W. H. (2000) Cardiac unloading alters contractility and calcium homeostasis in ventricular myocytes. *J. Mol. Cell. Cardiol.* **32**, 577–584
 45. Xydas, S., Rosen, R. S., Ng, C., Mercado, M., Cohen, J., DiTullio, M., Magnano, A., Marboe, C. C., Mancini, D. M., Naka, Y., Oz, M. C., and Maybaum, S. (2006) Mechanical unloading leads to echocardiographic, electrocardiographic, neurohormonal, and histologic recovery. *J. Heart Lung Transplant.* **25**, 7–15
 46. Yacoub, M. H., Tansley, P., Birks, E. J., Bowles, C., Banner, W. R., and Khaghan, A. (2001) A novel combination therapy to reverse end-stage heart failure. *Transplant. Proc.* **33**, 2762–2764
 47. Mohapatra, B., Vick, G. W., III, Fraser, C. D., Jr., Clunie, S. K., Towbin, J. A., Sinagra, G., and Vatta, M. (2010) Short-term mechanical unloading and reverse remodeling of failing hearts in children. *J. Heart Lung Transplant.* **29**, 98–104
 48. Terracciano, C. M., Miller, L. W., and Yacoub, M. H. (2010) Contemporary use of ventricular assist devices. *Annu. Rev. Med.* **61**, 31.1–31.16
 49. Soppa, G. K., Barton, P. J., Terracciano, C. M., and Yacoub, M. H. (2008) Left ventricular assist device-induced molecular changes in the failing myocardium. *Curr. Opin. Cardiol.* **23**, 206–218
 50. Ito, K., Nakayama, M., Hasan, F., Yan, X., Schneider, M. D., and Lorell, B. H. (2003) Contractile reserve and calcium regulation are depressed in myocytes from chronically unloaded hearts. *Circulation* **107**, 1176–1182
 51. Ogletree, M. L., Sweet, W. E., Talerico, C., Klecka, M. E., Young, J. B., Smedira, N. G., Starling, R. C., and Moravec, C. S. (2010) Duration of left ventricular assist device support: effects on abnormal calcium cycling and functional recovery in the failing human heart. *J. Heart Lung Transplant.* **29**, 554–561

Received for publication February 25, 2010.

Accepted for publication April 15, 2010.